Optimum Control of an Unstable Booster with Actuator Position and Rate Limits

BERNARD FRIEDLAND*
General Precision, Inc., Little Falls, N. J.

The general problem of designing an autopilot to achieve optimum response of a rigid aerodynamically unstable booster is considered. The vehicle is represented by a second-order linear model, and the actuator is represented by a first-order model having rate and position limits. The maximum principle of Pontryagin and its extension to bounded state variables are employed to obtain general conditions that the optimum control law must satisfy, and it is shown that operation at either maximum rate or maximum deflection is optimum when the performance measure is explicitly independent of the control. The switching surface for time-optimum control is calculated, and expressions are obtained for the maximum stability region. A readily implemented suboptimum control law was devised, and its performance was investigated by analog simulation. The results achieved showed that this suboptimum control law yields excellent transient response and realizes the maximum stability region.

Nomenclature

a	=	vehicle angle of attack
A_1, A_2	=	constants in autopilot realization
C	=	normalized rate limit
D	=	normalized position limit
F	=	vehicle thrust
F_D	=	drag force
F_L	=	lift force
g	=	integrand in performance index
H	=	Hamiltonian function
J	=	vehicle inertia
K	=	rate limit
K_1	=	actuator time constant
l_α	=	aerodynamic moment arm
l_c	=	control moment arm
M	=	vehicle mass
N_α	=	aerodynamic normal force
p_i	=	adjoint variables ($i = 1, 2, 3, 4$)
q_1	=	normalized position
q_2	=	normalized rate
q_3	=	normalized thrust deflection
s	=	complex frequency
t	=	time
T	=	final time
u	=	normalized control
v	=	velocity of vehicle normal to trajectory
V	=	vehicle forward speed
x, y	=	constants in autopilot realization
α	=	$1 - \sigma q_2$, normalized variable
β	=	$\sigma(q_1 + q_3)$, normalized variable
γ	=	σq_3, normalized variable
δ	=	thrust deflection
δ_c	=	thrust-deflection command
Δ	=	thrust-deflection limit
θ	=	vehicle attitude
μ_α	=	$N_\alpha l_\alpha / J$
μ_c	=	$F l_c / J$
σ	=	± 1
$\tau, \tau_1, \tau_2, \tau_f$	=	normalized times
ω	=	angular velocity of vehicle

Presented as Preprint 64-236 at the 1st AIAA Annual Meeting, Washington, D. C., June 29–July 2, 1964; revision received February 26, 1965. Much of this material was discussed with P. E. Sarachik of Columbia University who provided a number of useful comments. The analog simulation described in Sec. 4.3 was performed by S. Alexander and E. Toohey of the Flight Control Department, Aerospace Systems Division of General Precision, Inc.

* Principal Staff Scientist, Control, Aerospace Research Center. Member AIAA.

1. Introduction

THE design of an autopilot for an aerodynamically unstable booster is a challenging problem. When the actuator to be used to implement control motion is limited in amplitude and/or rate, the problem is compounded. The limits on the actuator capability combine with the inherent instability of the vehicle to yield a situation in which it is impossible to stabilize the vehicle for disturbances falling outside a given region (in state space). The best that can be done in this circumstance is to design an autopilot that achieves the maximum stability region. To attain this objective, it is necessary to consider the nonlinear effects due to the presence of the actuator limits: no linear analysis is capable of revealing the extent of the stability region. The determination of the extent of the region of stability, for processes having $2n$ real, equal and opposite (hence n unstable) characteristic roots with an actuator position limit, has been considered by Higdon and Cannon.[1] This investigation, however, did not treat rate limiting and was not concerned with optimum performance.

The design of an autopilot that achieves the maximum stability region and performs optimally within this region is a natural application of modern optimum control theory as it has evolved during the past several years. This theory reveals the structure of the optimum autopilot; moreover, the inherent instability of the vehicle in the model employed here has the fortuitous advantage of yielding a completely analytic solution for the optimum control law for minimum transient time.

When the motion of the vehicle is confined to a plane and the angular deviations and the component of velocity normal to the trajectory are small, the dynamic behavior can be approximated by the following differential equations[2]:

$$d\theta/dt = \omega$$

$$d\omega/dt = \mu_\alpha[\theta - (v/V)] + \mu_c\delta \qquad \mu_\alpha > 0$$

$$dv/dt = [(T + F_L)/M]\theta - [(F_D + F_L)/MV]v - (T/M)\delta$$

where θ is vehicle attitude, ω is attitude rate, v is velocity of vehicle normal to trajectory, and the other parameters are defined in the nomenclature. Although these parameters are generally time-dependent, experience has shown that in many problems their variation is slow enough to permit them to be treated as constants.

These equations are represented by the portion of the block diagram of Fig. 1 labeled "vehicle" and were used to evaluate the performance of the autopilot subsequently designed.

For analytical purposes, it was found convenient to introduce a further approximation that the velocity of the vehicle normal to the trajectory is negligible. This has the effect of reducing the dynamic equations to the following:

$$d\theta/dt = \omega \tag{1a}$$

$$d\omega/dt = \mu_\alpha\theta + \mu_c\delta \tag{1b}$$

Note that $\mu_\alpha > 0$ implies that the natural motion of the vehicle is unstable. The simplification afforded by replacing the original dynamic equations by (1) can be interpreted in the frequency domain as the cancellation of a pole at the origin by a real zero near the origin and the replacement of a positive and a negative pole by a pair of equal and opposite poles. For many systems this approximation is permissible; the validity of the approximation was verified in the simulation described later.

The control deflection δ is realized by means of an actuator whose dynamic behavior is represented by the first-order differential equation

$$\frac{d\delta}{dt} = \begin{cases} K_1(\delta_c - \delta) & |\delta_c - \delta| < K/K_1 \quad |\delta| < \Delta \\ K \operatorname{sgn}(\delta_c - \delta) & |\delta_c - \delta| \geq K/K_1 \quad |\delta| < \Delta \\ 0 & |\delta| = \Delta \end{cases} \tag{1c}$$

where δ is a deflection command generated by the autopilot. We also have the constraint

$$|\delta| \leq \Delta \tag{2}$$

Equation (1c) states that the actuator is linear when the difference between δ_c and δ is small, and it is represented by the transfer function $K_1/(s + K_1)$. However, the rate $\dot{\delta}$ cannot exceed a maximum value of K. When the deflection reaches a maximum magnitude of Δ, the motion ceases. Moreover, as indicated by (2), the deflection cannot exceed Δ in magnitude. The infinite slope of the nonlinear feedback in the actuator shown in Fig. 1 is necessary to insure that $\dot{\delta} = 0$ when $|\delta| = \Delta$ and represents the physical stops on the actuator motion.

It is convenient to normalize the equations of motion and constraint by the introduction of the following variables:

$$\left.\begin{array}{llll} q_1 = \mu_\alpha^{3/2}\theta/K\mu_c & \tau = \mu_\alpha^{1/2}t & & \\ q_2 = \mu_\alpha\omega/K\mu_c & C = \mu_\alpha^{1/2}/K_1 & u = \mu_\alpha^{1/2}\delta_c/K & \\ q_3 = \mu_\alpha^{1/2}\delta/K & D = \mu_\alpha^{1/2}/K & & \end{array}\right\} \tag{3}$$

Substitution of these into (1a–2) results in the following normalized differential equations:

$$dq_1/d\tau = q_2 \tag{4a}$$

$$dq_2/d\tau = q_1 + q_3 \tag{4b}$$

$$\frac{dq_3}{d\tau} = \begin{cases} (u - q_3)/C & |u - q_3| < C \quad |q_3| < D \\ \operatorname{sgn}[(u - q_3)/C] & |u - q_3| \geq C \quad |q_3| < D \\ 0 & |q_3| = D \end{cases} \tag{4c}$$

The constraint (2) is now expressed as

$$|q_3| \leq D \tag{5}$$

The objectives of the autopilot design are twofold: first, to achieve stability when possible, and second, to achieve optimum performance. To the latter end, we define a performance criterion

$$q_4(\tau_f) = \int_0^{\tau_f} g(q_1, q_2, q_3)\,d\tau \tag{6}$$

where τ_f is the normalized terminal time, either specified in advance or determined as the solution to the problem. The starting time is taken as zero [with no loss in generality, since (4) and (5) are autonomous]. To insure stability we require that

$$q_1(\tau_f) = q_2(\tau_f) = q_3(\tau_f) = 0 \tag{7}$$

Hence, if τ_f is finite, not only is stability insured, but also the transient is reduced to zero in the finite time $T = \tau_f/\mu_\alpha^{1/2}$ and remains zero thereafter in the absence of subsequent disturbances. Note that g is explicitly independent of the control u.

Thus, the problem to be solved is the following: minimize $q_4(\tau_f)$ for the process governed by the differential equations (4) subject to the constraint (5) and the terminal conditions (7). In this problem there is no constraint on the command deflection δ_c.

2. Structure of Optimum Autopilot

2.1 Application of Maximum Principle in Absence of Deflection Constraint

We first consider the problem in which the "state-variable" deflection constraint (5) is absent, since, as will be shown subsequently, the solution of this problem is necessary for the complete solution. In accordance with the theory developed by Pontryagin et al.,[3] we define a Hamiltonian function

$$H = \sum_{i=1}^{4} \frac{p_i dq_i}{d\tau} = p_1q_2 + p_2(q_1 + q_3) + p_3\varphi + p_4g \tag{8}$$

where p_i are so-called "adjoint" or "costate" variables and satisfy the adjoint differential equations

$$dp_i/d\tau = -\partial H/\partial q_i \qquad i = 1, 2, 3, 4, \tag{9}$$

and where

$$\varphi = \begin{cases} (u - q_3)/C & |u - q_3| < C \\ \operatorname{sgn}(u - q_3)/C & |u - q_3| \geq C \end{cases} \tag{10}$$

The main result of optimum control theory is Pontryagin's *maximum principle*, which asserts that one necessary condition for the optimum control function $u(\tau)$ is that the Hamiltonian H be maximum with respect to u.

The only term in the Hamiltonian (8) that depends on u is φ, and thus, H is maximized by making φ as large as possible when $p_3 > 0$ and as small as possible when $p_3 < 0$. (When $p_3 \equiv 0$ the maximum principle gives no information about the control. This is a singular situation, which is excluded from the present problem by assumption.) Evidently, the largest possible value of φ is unity and is attained when $u - q_3 \geq C$. Thus, for optimum performance we must have

$$u \geq q_3 + C \quad \text{when} \quad p_3 > 0 \tag{11a}$$

Likewise the smallest possible value of φ is -1 and is attained when $u - q_3 \leq -C$. Thus we must have

$$u \leq q_3 - C \quad \text{when} \quad p_3 < 0 \tag{11b}$$

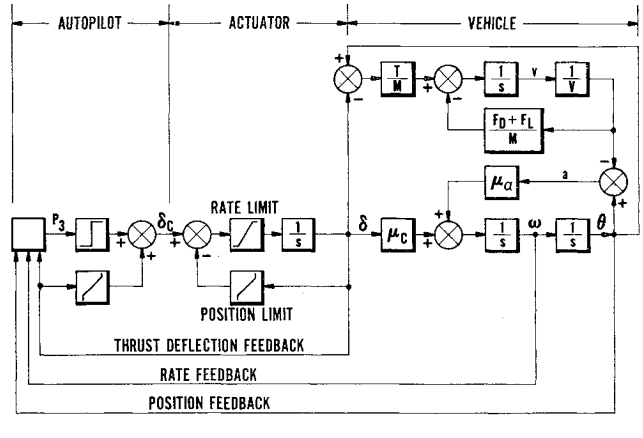

Fig. 1 Block diagram of control system.

This implies that the optimum actuation always takes place using either the maximum positive or the maximum negative rate.

The switching from maximum positive to maximum negative rate and vice versa occurs at the instants that $p_3 = 0$. Thus, the optimum control law is completed by specifying p_3 as a function of the state (q_1, q_2, q_3).

To determine this function, the adjoint equations (9) are used:

$$dp_1/d\tau = -\partial H/\partial q_1 = -p_2 - p_4 \partial g/\partial q_1 \quad (12a)$$

$$dp_2/d\tau = -\partial H/\partial q_2 = -p_1 - p_4 \partial g/\partial q_2 \quad (12b)$$

$$dp_3/d\tau = -\partial H/\partial q_3 = -p_1 - p_4 \partial g/\partial q_3 \quad (12c)$$

$$dp_4/d\tau = -\partial H/\partial q_4 = 0 \quad (12d)$$

This set of differential equations, together with the equations of motion (4) and

$$dq_4/d\tau = g(q_1, q_2, q_3) \quad (13)$$

comprise a system of eight differential equations that must be integrated with appropriate boundary conditions to yield the optimum control law. The boundary conditions are $q_i(0) = q_{i0}$; $q_i(\tau_f) = 0, i = 1, 2, 3$; $q_4(0) = 0$; and $p_4(\tau_f) = -1$.

The first three conditions specify the arbitrary normalized state in which the process can be at $t = 0$, and the fourth indicates that the integral in (6) is zero at $t = 0$. The next three conditions are the requirement that the transient be reduced to zero at $\tau = \tau_f$, and the last is a condition that results directly from the maximum principle. [Incidentally, the last equation and the fourth, together with (12d) and (13), do not influence the final result.] The equations must be integrated with u given by (11).

2.2 Effect of Deflection Constraint

In the previous section, we have considered the case in which the deflection constraint (5) is absent, i.e., when only the rate is limited. When the deflection constraint is present, the solution previously obtained may not be valid. In particular, it is invalid for those initial conditions that would result in a solution that does not satisfy (5), that is, when the maximum rate commands are applied long enough to cause a deflection limit to be exceeded. The theory with which this problem can be treated is attributed to Gamkrelidze,[3,4] Berkovitz,[5] and Bryson, Denham, and Dreyfus.[6]

The optimum trajectory (in state space) consists of two types of segments: 1) segments along which the constraint (5) is satisfied by a strict inequality, i.e.,

$$|q_3| < \mu_\alpha^{1/2}\Delta/K = D \quad (14)$$

and 2) segments along which the constraint is satisfied with the equals sign, i.e.,

$$h(q_3) = |q_3| - D = 0 \quad (15)$$

Case 1

Those segments of the trajectory along which (14) holds satisfy the maximum principle. This means that the optimum input command satisfies (11) and results in operation at maximum positive or negative rate and, also, that the adjoint variables $p_i (i = 1, \ldots, 4)$ satisfy the adjoint equations (12).

Case 2

For the segments of the trajectory which satisfy (15), it is necessary that $dq_3/d\tau = 0$; this implies that $u - q_3 = 0$. (The infinite slope of the nonlinear characteristic of Fig. 1 is a schematic representation of this.) In this case, it is not possible to maximize the Hamiltonian (8) with respect to the control variable u. Instead we must have $u = q_3$ and

$$\partial H/\partial u = \lambda(\partial/\partial u)(dh/d\tau) \quad (16)$$

where H is evaluated in the neighborhood of $u - q_3 = 0$, i.e.,

$$H = p_1 q_2 + p_2(q_1 + q_3) + p_3 C^{-1}(u - q_3) + p_4 g \quad (17)$$

and where

$$\frac{dh}{d\tau} = \sum_{i=1}^{3} \frac{\partial h}{\partial q_i}\frac{dq_i}{d\tau} = \frac{u - q_3}{C} \quad (18)$$

On using (17) and (18), we obtain

$$\lambda = p_3 \quad (19)$$

The Lagrange multiplier λ just calculated is reflected in a modified system of adjoint equations:

$$\frac{dp_i}{d\tau} = -\frac{\partial H}{\partial q_i} + \lambda \frac{\partial}{\partial q_i}\left(\frac{dh}{d\tau}\right) \qquad i = 1, 2, 3, 4 \quad (20)$$

In view of (18), the first two and last of (20) are the same as (12a, 12b, and 12d), respectively. As for the third, we have, from (17),

$$\frac{dp_3}{d\tau} = -\frac{\partial H}{\partial q_3} + \lambda \frac{\partial}{\partial q_3}\left(\frac{dh}{d\tau}\right) = -p_2 + \frac{p_3}{C} - p_4 \frac{\partial g}{\partial q_3} - \frac{\lambda}{C} \quad (21)$$

But from (19) $\lambda = p_3$. Hence (21) is identical to (12c). Thus (12a–12d) govern the adjoint variables everywhere along an optimum trajectory.

To preserve the continuity of the Hamiltonian (8), as required by the theory,[6] it is necessary that the adjoint variable p_3 change discontinuously at the instants at which the trajectory enters the deflection-limited region from the rate-limited region. Let τ_i' denote these instants; then we must have

$$p_3(\tau_i'^{-}) = 0 \qquad p_3(\tau_i'^{+}) = \mu = \text{const} \quad (22)$$

All other components $p_i(\tau)$ of the adjoint vector are continuous everywhere along an optimum trajectory. At the instants at which the trajectory returns from the deflection-limited to the rate-limited region, it is required that $p_3(\tau_i) = 0$, just as in the case in which there are no deflection constraints.

3. Minimum-Response-Time Design

3.1 Deflection Constraint Absent

We now consider the design of the autopilot to minimize the time-of-response τ_f. This is accomplished by choosing $g(q_1, q_2, q_3) = 1$, whence the performance criterion (6) reduces to

$$q_4(\tau_f) = \int_0^{\tau_f} d\tau = \tau_f$$

In this case, the adjoint equations (12) become simply $dp_1/d\tau = -p_2$, $dp_2/d\tau = -p_1$, and $dp_3/d\tau = -p_2$. The integrals of these equations are

$$p_1(\tau) = p_{10}\cosh\tau - p_{20}\sinh\tau \quad (23a)$$

$$p_2(\tau) = -p_{10}\sinh\tau + p_{20}\cosh\tau \quad (23b)$$

$$p_3(\tau) = p_{30} + p_{10}(\cosh\tau - 1) - p_{20}\sinh\tau \quad (23c)$$

where $p_{10} = p_1(0)$, $p_{20} = p_2(0)$, and $p_{30} = p_3(0)$. It is readily established that $p_3(\tau)$ as given by (23) has at most two real roots, say τ_1 and τ_2 ($\tau_2 > \tau_1$). Consequently, in accordance with the result established in Sec. 2 by use of the maximum principle,

$$\frac{dq_3}{d\tau} = \begin{cases} \sigma & 0 \le \tau \le \tau_1 \\ -\sigma & \tau_1 \le \tau \le \tau_2 \\ \sigma & \tau_2 \le \tau \le \tau_f \end{cases}$$

where $\sigma = \text{sgn} p_{30}$ with discontinuities at τ_1 and τ_2. Integrating, we obtain

$$q_3(\tau) = \begin{cases} q_{30} + \sigma\tau & 0 \le \tau \le \tau_1 \\ q_{30} + 2\sigma\tau_1 - \sigma\tau & \tau_1 \le \tau \le \tau_2 \\ q_{30} + 2\sigma(\tau_1 - \tau_2) + \sigma\tau & \tau_2 \le \tau \le \tau_f \end{cases} \quad (24)$$

Upon substituting (24) into (4a) and (4b), integrating from $\tau = 0$ to $\tau = \tau_f$, and imposing the requirement that $q_1(\tau_f) = q_2(\tau_f) = 0$, the following expressions are obtained:

$$q_{10} + q_{30} = [q_{30} + \sigma\tau_f - 2\sigma(\tau_2 - \tau_1)]\cosh\tau_f + \sigma[-\sinh\tau_f + 2(\sinh\tau_2 - \sinh\tau_1)] \quad (25)$$

$$-q_{20} - \sigma = [q_{30} + \sigma\tau_f - 2\sigma(\tau - \tau_1)]\sinh\tau_f + \sigma[-\cosh\tau_f + 2(\cosh\tau_2 - \cosh\tau_1)]$$

It is also required that $q_3(\tau_f) = 0$, or, from (24),

$$q_{30} + 2\sigma(\tau_1 - \tau_2) + \sigma\tau_f = 0 \quad (26)$$

and this reduces (25) to

$$\sigma(q_{10} + q_{30}) = -\sinh\tau_f + 2(\sinh\tau_2 - \sinh\tau_1) \quad (27)$$

$$-\sigma q_{20} - 1 = -\cosh\tau_f + 2(\cosh\tau_2 - \cosh\tau_1) \quad (28)$$

Equations (26–28) give three relations between q_{10}, q_{20}, and q_{30} (and $\sigma = \mathrm{sgn}p_{30}$); and τ_1, τ_2, and τ_f could be obtained as functions of q_{10}, q_{20}, q_{30}, and $\mathrm{sgn}p_{30}$. The first two can then be substituted into (25) from which a single relation between p_{30} and q_{10}, q_{20}, and q_{30} can be obtained. Since q_{10}, q_{20}, and q_{30} are arbitrary, this relation is valid at any starting time. Consequently, omission of the subscripts 0 on p_{30} and q_{10}, q_{20}, and q_{30} yields the required relation between p_3 and q_1, q_2, and q_3 at any time.

Calculation of switching surface

In this problem, the expression for p_3 as a function of the state (q_1, q_2, q_3) is not required at every point in the state space; any function that has the same sign as p_3 will be equally good, since the control law depends only on the sign of p_3. Thus, we require only an expression that is zero when $p_3 = 0$. The surface thus obtained is called a "switching surface." On one side of the surface, the maximum positive rate is used; on the other, the maximum negative rate is used.

The switching surface is obtained by noting that switching occurs at a state for which $\tau_1 = 0$. Thus, setting $\tau_1 = 0$ in (26–28), we obtain

$$\sigma q_3 - 2\tau_2 + \tau_f = 0 \quad (29a)$$

$$\sigma(q_1 + q_3) = -\sinh\tau_f + 2\sinh\tau_2 \quad (29b)$$

$$-\sigma q_2 + 1 = -\cosh\tau_f + 2\cosh\tau_2 \quad (29c)$$

which is a parametric representation for the switching surface; τ_2 and τ_f are the parameters. Elimination of τ_2 and τ_f in (29a–29c) results in

$$(\alpha^2 - \beta^2)^2 - 6(\alpha^2 - \beta^2) + 8(\alpha\cosh\gamma - \beta\sinh\gamma) - 3 = 0 \quad (30)$$

where

$$\alpha = 1 - \sigma q_2 \qquad \beta = \sigma(q_1 + q_3) \qquad \gamma = \sigma q_3 \quad (31)$$

The switching surface has the appearance shown in Fig. 2. The lightweight lines are curves of constant response time τ_f and are thus the intersections of the state-space isochrones with the switching surface.

Maximum stability region†

The maximum region of stability is defined here as the set of states outside of which it is impossible to reach the origin in any finite time. The boundary of this region is obtained by letting $\tau_f \to \infty$ in (29). Since q_3 is to remain finite, as τ_2, $\tau_f \to \infty$, we obtain $\sinh\tau_f$, $\cosh\tau_f \sim e^{\tau_f}/2$ and $\sinh\tau_2$, $\cosh\tau_2 \sim e^{\tau_2}/2$ or $\sigma(q_1 + q_3) \sim -e^{\tau_f}/2)e^{\tau_2}$ and $1 - \sigma q_2 \sim -e^{\tau_f}/2 + e^{\tau_2}$. Since the right-hand sides are asymptotically

† In Ref. 1, the term "maximum region of controllability" is employed.

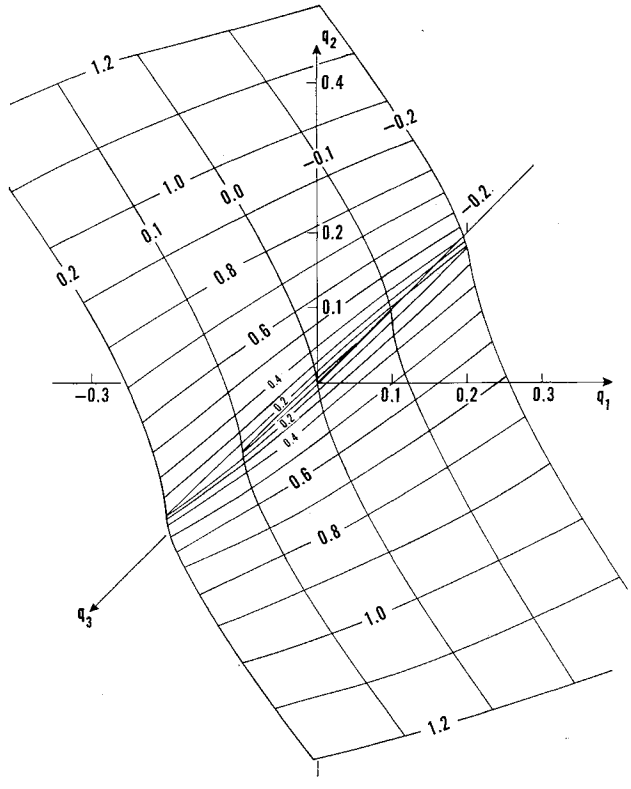

Fig. 2 Optimum switching surface, rate-limited.

equal, the boundary of the region is given by

$$1 - \sigma q_2 = \sigma(q_1 + q_3) \quad \text{or} \quad q_1 + q_2 + q_3 = \sigma = \pm 1 \quad (32)$$

Thus, the maximum region of stability is the region bounded by a pair of planes in the (q_1, q_2, q_3) space.

3.2 Effect of Deflection Constraint

With the deflection constraint present, the switching surface derived in the previous section can be expected to require modification. As discussed in Sec. 2.2, any optimum trajectory in the state space may be broken into segments such that on each segment either $|q_3| < D$, in which case the maximum principle applies, and the rate is either at its maximum or minimum value, or else $|q_3| = D$, i.e., $q_3 = \pm D$. To maintain this condition, it is required that the input $\delta_c - \delta$ to the integrator in Fig. 1 drop to zero. This is automatically accomplished by the stop in the physical system independent of the command input δ_c. However, if the physical stops were absent, or if it is desirable to avoid forcing the actuator against its stop, then a command input should be generated to keep $dq_3/d\tau = 0$ when $q_3 = \pm D$, i.e., one should make $\delta_c = \mp\Delta$ when $\delta = \pm\Delta$.

Evidently, if the deflection limit Δ is large (with respect to the initial conditions), then this limit may be ignored, since the transient will never force saturation. Hence, for a region (whose size depends on Δ) surrounding the origin in state space, the switching surface calculated in the previous section will remain valid. The following question then arises: Does this region cover the entire portion of the state space lying inside the stability limits (32) and in the slab $-D \leq q_3 \leq D$? The answer to this question is negative. Thus, it becomes necessary to determine the extent of the validity of the previously calculated switching surface and then to determine the expression for the switching surface outside this region.

Region of validity of rate-limited switching surface

The switching surface given by (30) is valid as long as the trajectories that result have $|q_3(\tau)| \leq D$, $0 \leq \tau \leq \tau_f$. Since

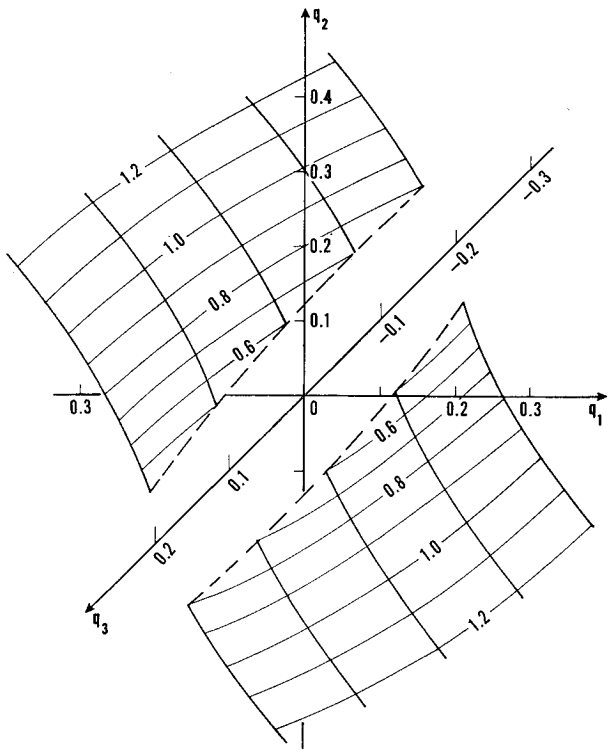

Fig. 3 Optimum switching surface, deflection- and rate-limited, $D = 0.3$.

$q_3(\tau)$ reaches its maximum and minimum values on the switching surface, (31) is valid when

$$|q_3(\tau_1)| \leq D \qquad \text{and} \qquad |q_3(\tau_2)| \leq D$$

There is no loss in generality in assuming $\tau_1 = 0$, i.e., that the trajectory to be examined starts on the switching surface. Thus, we must satisfy $|q_3| \leq D$, and from (24)

$$|\tau_2 - \sigma q_3| \leq D \tag{33}$$

where q_3 is any state on the switching surface. The first condition is evident and needs no further explanation. Our attention, therefore, is confined to (33). However, since $\tau_2 - \sigma q_3 = \tau_f - \tau_2 \geq 0$, the magnitude signs can be omitted. Thus, the region in which (30) is valid is given by

$$\tau_2 - \sigma q_3 \leq D \tag{34}$$

which, it can be shown, is equivalent to

$$1 - e^{-\gamma}(\alpha + \beta) \leq (e^D - 1)^2 \tag{35}$$

Thus, the region in which the switching surface of (30) is valid is

$$q_1 + q_3 - 1 - e^{-q_3}[(e^D - 1)^2 - 1] \leq q_2 \leq q_1 + q_3 + 1 + e^{q_3}[(e^D - 1)^2 - 1] \tag{36}$$

For any state (q_1, q_2, q_3) on the original switch surface which does not satisfy (36), a different surface must be found.

Rate- and position-limited switching surface

The procedure used in Sec. 3.1 to calculate the switching surface when only the rate limit is present will be repeated here. The basis of this calculation is the assumption that the initial state lies upon the switching surface, which is then determined as the locus of states that satisfy the terminal conditions $q_1(\tau_f) = q_2(\tau_f) = q_3(\tau_f) = 0$, when the optimum control u is applied for $0 \leq \tau \leq \tau_f$.

It is evident that, if the state is initially on the switching surface ($\tau_1 = 0$), then, for $\tau > 0$,

$$q_3(\tau) = \begin{cases} q_{30} - \sigma\tau & 0 \leq \tau \leq \tau_2' \\ -\sigma D & \tau_2' \leq \tau \leq \tau_2 \\ -\sigma D - \tau + \tau_2 & \tau_2 \leq \tau \leq \tau_f \end{cases} \tag{37}$$

where τ_2' is the instant at which the position limit is reached and is given by

$$\tau_2' = \sigma q_3 + D \tag{38}$$

Substitution of (37) into (4a) and (4b), integration, and use of the terminal condition

$$D - \tau_f + \tau_2 = 0 \tag{39}$$

results in the following parametric equations for the required switching surface:

$$\begin{aligned} \sigma(q_1 + q_3) &= -\sinh\tau_f + \sinh\tau_2' + \sinh\tau_2 \\ -\sigma q_2 + 1 &= -\cosh\tau_f + \cosh\tau_2' + \cosh\tau_2 \end{aligned} \tag{40}$$

Note that these equations reduce to those in which only rate-limiting is present as expressed by (29) when $\tau_2' = \tau_2$. To obtain the required switching surface, τ_2' and τ_f as given by (38) and (39), respectively, are substituted into (40), and the parameter τ_2 is then eliminated. The result of this calculation is

$$\alpha^2 - \beta^2 - 2\alpha\cosh(D + \gamma) + 2\beta\sinh(D + \gamma) + 2\cosh D - 1 = 0 \tag{41}$$

where α, β, and γ are defined in (31). On using these definitions in (41), the following expression for the switching surface is obtained directly in terms of q_1, q_2, and q_3:

$$q_2^2 - 2\sigma q_2[1 - \cosh(D + \sigma q_3)] - (q_1 + q_3)\sinh(D + \sigma q_3) + 2\cosh D - 2\cosh(D + \sigma q_3) = 0 \tag{42}$$

The corresponding switching surface in the applicable region (36) is shown in Fig. 3.

Maximum stability region

As in the case of only rate-limiting, the set of points in the (q_1, q_2, q_3) space which can be brought to the origin in a finite time is bounded by the surfaces obtained by letting τ_f and τ_2 in (40) approach infinity but with τ_2' given by (38) remaining finite. The asymptotic expressions are

$$\begin{aligned} \sigma(q_1 + q_3) - \sinh\tau_2' &\sim (e^{\tau_2} - e^{\tau})/2 \\ 1 - \sigma q_2 - \cosh\tau_2' &\sim (e^{\tau} - e^{\tau_f})/2 \end{aligned}$$

whence the required asymptotes are given by

$$\sigma(q_1 + q_2) - \sinh\tau_2' = 1 - \sigma q_2 - \cosh\tau_2'$$

or, using $\tau_2' = \sigma q_3 + D$,

$$\sigma(q_1 + q_2 + q_3) = 1 - e^{(\sigma q_3 + D)} \tag{43}$$

where $\sigma = \pm 1$.

4. Realization of Optimum and Suboptimum Control Laws

4.1 General Character of Autopilot

It is recalled that the minimum-time solution (as well as the optimum solution for other performance criteria) requires that the actuator be operated at maximum (positive or negative) rate until the position limits are attained. Thus, the only problem is to determine those states for which the deflection should be positive and those for which it should be negative. The regions are separated by a switching surface,

which, for minimum-time response, has been calculated in the previous section.

From the standpoint of realization, this result has several important implications. It is seen that the negative linear feedback in the actuator is not needed, since the actuator should always be operated in the rate-saturated condition, unless the position limits are attained, in which case the rate is zero. This fact, however, does not imply that there is no feedback of the actuator position, but rather that the feedback is to be furnished through the autopilot, since the switching surface depends not only on $q_1 \propto \theta$ and $q_2 \propto \omega$ but also on $q_3 \propto \delta$. This suggests that the autopilot be integrated with the actuator; if this integration is not possible, then the actuator position will have to be sensed in order to realize the optimum control law. Integration of the autopilot with the actuator would also permit the deflection command signal to be removed when the position limit is reached, until the state is reached at which the direction of the deflection should be reversed. This would prevent the mechanical stressing of the stops and would also conserve power.

The absence of a requirement for proportional control is another noteworthy feature, since it permits the use of relatively unsophisticated (and hence more reliable) components. If a hydraulic actuator is employed, for example, a proportional control valve (a component that is relatively unreliable) can be replaced with a system of solenoid valves. (It would be necessary for this system to have an accurate null characteristic; a small "proportional" region in the vicinity of the null might also be useful in connection with suboptimum control, but the slope of this region need not be controlled accurately; in fact, the region need not be linear.)

4.2 Suboptimum Control Law

The switching surfaces calculated in the previous section, given by (30) and (42) with the equation of transition (36), can be realized to any specified accuracy with a digital computer or by nonlinear analog components. The question arises, however, whether the realization of the exact optimum control law is warranted in view of the equipment complexity such a realization would entail. The following considerations should be taken into account:

1) The model upon which the theoretical calculations are based is only approximate. The actual process is governed by a system of nonlinear differential equations of much higher order.

2) Even if the model were accurate, the parameters μ_α and μ_c are generally not known with complete accuracy. This means that the transformation from the physical state variables (θ, ω, δ) to the normalized variables (q_1, q_2, q_3) may be in error by as much as 10% and possibly even more. Thus, even when the price of getting the exact switching law in terms of q_1, q_2, and q_3 is paid, the switching law from the physical state variables will generally be in error by as much as 10%.

In view of these considerations, one is led to seek a simple way of implementing a suboptimum switching surface that comes within, say, 10% of the exact surface and results in good stability. In view of the shape of the exact switching surfaces of Figs. 2 and 3, it seems that a suitable suboptimum switching surface can be constructed by the use of segments of planes.

Table 1 Initial conditions for simulation

Transient	Initial conditions		
	q_1	q_2	q_3
a	−0.506	0.0	0.0
b	−2.08	2.48	0.0
c	0.0	0.446	0.0
d	0.221	0.178	0.0

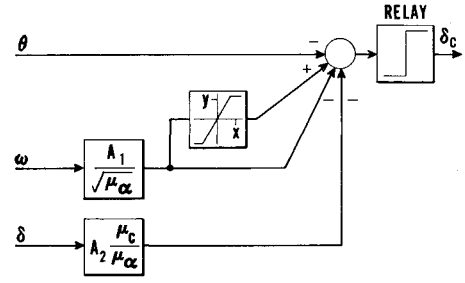

Fig. 4 Realization of suboptimum autopilot.

A very simple planar approximation can be realized by the use of an autopilot illustrated in Fig. 4. This configuration requires only a single nonlinearity. Inspection of the exact switching surface indicates that reasonable ranges for the constants x and y (which govern the slope and breakpoint of the nonlinearity) and the constants A_1 and A_2 should be

$$0.1 < x < 0.8 \qquad 0 < y/x < 1$$
$$0.8 < A_1 < 1.2 \qquad 0 < A_2 < 0.5 \tag{44}$$

4.3 Simulated Performance

To evaluate this suboptimum control law, an analog simulation was performed. After a bit of experimentation, the following settings of the constants were found to give very good performance for $D = 0.709$:

$$x = 0.5 \qquad y = 0.25 \qquad A_1 = 1.0 \qquad A_2 = 0.2 \tag{45}$$

Oscillograms of the response for the simplified model ($v \equiv 0$) with four sets of initial conditions, tabulated in Table 1, are given in Fig. 5. Note that the vertical scale for q_1 and q_2 is changed in each oscillogram.

The difference between the exact optimum response and the suboptimum response is reflected in the residual amount of q_3 (proportional to δ) after the major portion of the transient has subsided. It is observed that this quantity is indeed quite small. There is steady-state "dither" in the deflection command (characteristic of this type of approximation) because of rapid switching about the approximate surface in the neighborhood of the origin.

A further indication of the performance of the suboptimum control law is the extent of the stability region. The analog simulation was used to obtain this region experimentally with the results given in Fig. 6. The curves connecting the experimentally obtained points are those given by (43). It is seen that this suboptimum controller realizes virtually the entire region in which stability is possible. This fact may be more important than the exact shape of the response curves.

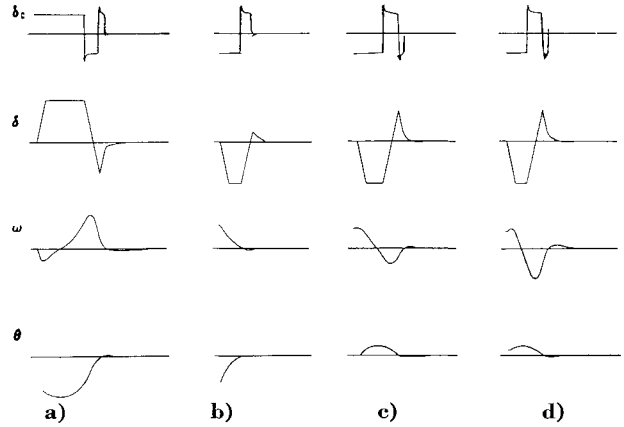

Fig. 5 Transient response, simplified model, $D = 0.709$.

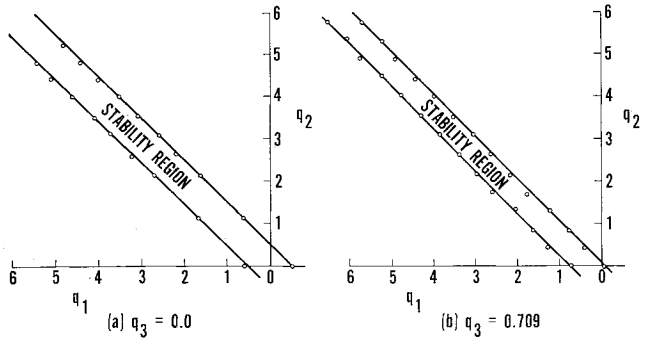

Fig. 6 Stability regions, $D = 0.709$.

The performance of this autopilot with the more accurate dynamical model of the vehicle shown in Fig. 1 was also investigated for the same initial conditions shown in Table 1 and with $v(0) = 0$. For this simulation, the vehicle parameters were approximately as follows:

$$(T + F_L)/M \approx 170 \text{ ft-sec}^{-2}$$
$$(F_D + F_L)/MV \approx 0.01 \text{ sec}^{-1}$$
$$T/M \approx 150 \text{ ft-sec}^{-2}$$

which are reasonably representative actual vehicles. The results of this simulation are shown in Fig. 7. Comparison of Fig. 7 with Fig. 5 shows that the response of the more accurate model is substantially the same as that of the simplified model. The maximum of the ratio v/V is about 0.01, which further justifies the approximation that $v = 0$.

The maximum region of stability was also investigated by simulation, and it was found that the stability is not compromised by the inclusion of the additional dynamics.

In view of these results, the conclusion is inescapable that this suboptimum control law is entirely adequate for all practical purposes; any more accurate implementation would appear to be of academic interest only.

5. Summary and Conclusions

By means of the straightforward application of optimum control theory to a simplified dynamic model, the exact expression for the time-optimum control law for a rigid aerodynamically unstable booster with actuator position and rate limits has been obtained. A simple suboptimum control law, which appears to give excellent dynamic response and maximum stability, has been found and is consistent with the accuracy of the model and the knowledge of its parameters.

Before the recommendation can be made to utilize this control law, however, it would be necessary to obtain favorable answers to a number of additional questions, such as the following:

1) In view of the approximations employed in the model, will the control law be satisfactory when a more realistic model of the vehicle (possibly including bending effects and time-varying parameters) is employed?

2) Can the high-frequency dither in the deflection command, which causes a ripple in the steady-state deflection, excite a bending mode in the vehicle? If so, can an arrangement, such as low-pass filter between δ_c and the actuator input, be devised to eliminate this effect?

3) The design was based on the requirement of reducing the error due to initial conditions to zero as fast as possible, rather than on good following of attitude commands. Whereas the step response is identical to that in which there is only an initial position error, the response to a time-varying input, such as the system might be required to follow, should be evaluated. The response of the system to a ramp attitude command was investigated in the simulation and found to be excellent.

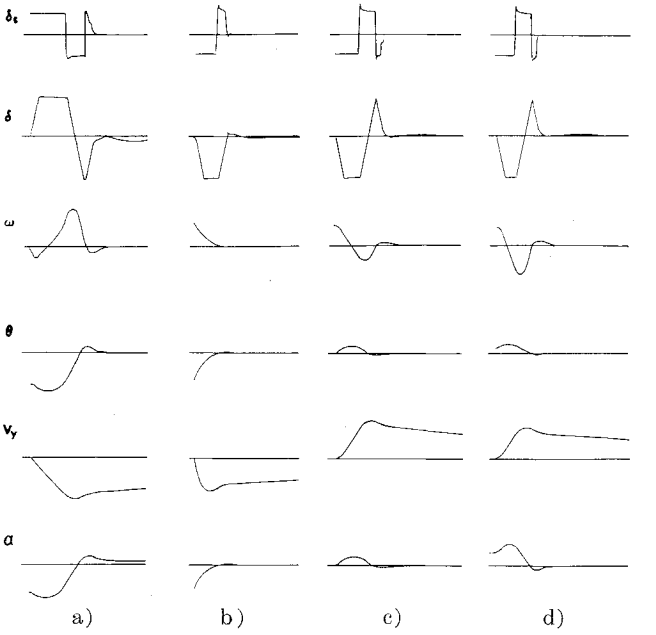

Fig. 7 Transient response, accurate model, $D = 0.709$

References

[1] Higdon, D. T. and Cannon, R. H., Jr., "On the control of unstable multiple-output mechanical systems," American Society of Mechanical Engineers Paper 63-WA-148 (November 17–22, 1963).

[2] Pitman, G. R., Jr. (ed.), *Inertial Guidance* (John Wiley and Sons, Inc., New York, 1962), p. 275.

[3] Pontryagin, L. S., Boltyanskii, V. G., Gamkrelidze, R. V., and Mishchenko, E. F., *The Mathematical Theory of Optimal Processes* (Interscience Publishers, Inc., New York, 1962).

[4] Gamkrelidze, R. V., "Optimal control processes with bounded phase coordinates," Izv. Akad. Nauk, USSR, Ser. Mat. **24**, 315–356 (1960).

[5] Berkovitz, L. D., "On control problems with bounded state variables," J. Math. Anal. Appl. **5**, 488–501 (1962).

[6] Bryson, A. E., Jr., Denham, W. F., and Dreyfus, S. E., "Optimal programming problems with inequality constraints, I: Necessary conditions for extremal solutions," AIAA J. **1**, 2544–2550 (1963).